GREEN ROOF RETROFITS: COMBINED SIMULATIONS TO ASSESS THE OUTDOOR MICROCLIMATE BENEFITS AND THE ENERGY SAVINGS

Umberto Berardi
Department of Architectural Science, Ryerson University
350 Victoria Street, Toronto, Ontario, M5B 2K3, Canada
uberardi@ryerson.ca

ABSTRACT

This paper focuses on the benefits on the local microclimate and the building energy saving resulting from green roof retrofits. The research investigates a case study located in a university campus in Toronto, Canada. After having completed a detailed energy audit of the building, the benefits resulting from the installation of an extensive green roof were assessed. Firstly, a virtual microclimate model allowed to simulate the effects of the green roof over the outdoor microclimate. Then, the building energy model allowed used to compare the energy savings of different green roof design options. Results indicate that increasing the leaf area index would leads to an increased cooling effect up to 0.4˚C during the day at pedestrian level. The green roof retrofit resulted in a building energy demand reduction by 3%, and in significantly improved indoor comfort levels on the floor immediately below the green roof.

INTRODUCTION

Green roofs offer many environmental benefits including stormwater flow reduction, air quality improvements, building energy saving, and mitigation of urban heat island (UHI) effects (Banting et al., 2005; Berardi et al., 2014). Given their commonly recognized benefits, the city of Toronto has adopted the Green Roof By-law, which requires the construction of vegetated roofs on all new developments with a gross floor area greater than 2,000m^2 (City of Toronto, 2015). Given to this policy, from 2010 to 2015, over 196,000m^2 of green roofs have been constructed in Toronto. The increasing attention towards green roofs is also supported by the Toronto Eco-Roof Program, which guarantees an incentive of $75 per m^2 for existing buildings and new buildings not subject to the Green Roof By-law (City of Toronto, 2015).

More urban vegetation is a fundamental aspect of the UHI mitigation policies promoted over the last years in Toronto, as well as across other Canadian cities. In fact, although commonly considered a cold country, episodes of extreme heat are becoming common in Canada. Over the last two decades, the Natural Resources Canada has used air temperature and surface temperature measurements collected from satellite imagery to characterize the microclimatology across Toronto and to assess the UHI effects (Wieditz and Penney, 2007, Maloley, 2009, Wang et al., 2016). Thermal images of surface temperatures have illustrated the increasing UHI effect over Toronto, and the importance to promote more stringent policies for its mitigation.

In an urban environment where available ground space is limited, roofs offer a substantial area for the implementation of UHI mitigation strategies, such as green roofs. A study by Ryerson University researchers estimated that a roof surface of about 50 million m^2 is available for green roof applications in Toronto, and that the implementation of these green roofs would have an annual public cost saving of $37 million for the city (Banting et al., 2005). The study assumed an additional building energy saving of 4.15kWh/m^2/year obtained through to green roofs, which would result in additional $21 million per year saving for building private owners.

Wang et al. (2015) recently investigated the impact of various UHI strategies in Toronto. Microclimate simulations showed that increasing the amount of vegetation had the largest impact on UHI mitigation compared to cool pavements and cool roofs. However, combining all these three UHI mitigation strategies, it would be possible to reduce the air temperature by 0.8˚C at mid-day and 0.6˚C at mid-night in the summer.

In retrofit projects, green roofs are generally built to enhance the energy saving of the buildings (Saadatian et al., 2013, Berardi et al., 2014), although the resulting increase in the thermal capacity of green roofs compared to traditional roofs, if not controlled, may also raise the building cooling and heating loads (Castleton et al., 2010).

So far, only a few studies have also looked at the capability of green roofs retrofits as a measure to reduce the urban canyon temperatures (Alexandri and Jones, 2008, Parizotto and Lamberts, 2011). A recent review by Santamouris (2014) found that the UHI mitigation potential of green roofs is highly dependent on the climate, roof U-value, and latent heat loss.

The present paper represents one of the first examples where energy and microclimate benefits of the green roofs are combined together and evaluated at the microscale of a single (large) building block. The paper will focus on a retrofit application and, although green roofs have mostly been considered in warm climates, this paper will look at the benefits in the cold climate of Toronto.

METHODOLOGY

Microclimate simulations were performed using ENVI-met 4.0, a three-dimensional computational fluid dynamics non-hydrostatic S.V.A.T. (soil, vegetation, atmosphere, and transfer) model. This program models the surface-plant-air interactions in urban environments, has been extensively validated and used in recent years (Ozkeresteci et al., 2003, Bruse, 2015, Wang et al., 2016). The program also simulates the flows around buildings, heat and vapor transfer at the urban surfaces, turbulence, exchanges of energy and mass between vegetation and its surroundings, and simple chemical reactions.

The main input parameters of ENVI-met simulations include weather conditions, initial soil wetness and temperature profiles, structures and physical properties of urban surfaces, and plants. Combining Reynolds averaged Navier–Stokes equations and the advection diffusion equation, ENVI-met allows to calculate the air temperature, water vapour pressure, relative humidity, wind velocity, and mean radiant temperature (MRT) (Bruse, 2015).

In ENVI-met, the soil model is organized in layers: heterogeneous surface types are simulated assigning to each grid cell a different thermodynamic and hydraulic conductivity, and albedo value. Vegetation is modelled for its evapotranspiration processes, shadow, and drag effects. ENVI-met carries out calculation in regards to both shortwave and long-wave radiation fluxes with respect to shading, reflection, and re-radiation from buildings and vegetation. The temperatures of the ground and building surfaces are finally calculated from an energy balance of differential equations solved using the finite difference method.

ENVI-met has a typical resolution of 0.5 m to 10m in space, and 10 seconds in time. A simulation should typically be carried out for at least 6 hours, but a 24 hours period is more usual. The optimal time to start a simulation is at night or sunrise, so that the simulation follows the solar radiation daily increase. In this paper, the model was simulated from 4am of August 15th to 4am of August 16th, using the local weather station data reported in Table 1 as initial boundary conditions. Only summer time was considered as prior studies showed negligible impact of the vegetation on winter outdoor comfort in downtown Toronto (Wang et al., 2016).

Table 1. Initial conditions for ENVI-met simulations.

Parameter	Input value
Start date	August 15th
Start time	4:00 am
Simulation time	24 hours
Wind direction	South-West (225°)
Wind speed (10m)	1.39 m/s
Specific humidity (2500m)	7.0 g/kg_{da}
Relative humidity (2m)	68.6%

ENVI-met requires an area input file with a 3-dimensional geometry. In this study, the geometrical model had dimensions of 220.5(x) x 217(y) x 60(z) m (with z being the vertical axis), with cell grids of 49x62x30. The total height of the model was significantly higher that the building height. Moreover, three nesting grids were implemented into the model in order to increase the accuracy around the borders. The ENVI-met model included the near buildings in order to calibrate and validate the as-it-is model using local weather stations (Fig.1).

For the placement of the vegetation into the model, the Ryerson Park-trees database was used (UFRED, 2015). This database provides information on the tree species, location, and attributes, such as tree height or crown radius.

For the analysis, the simulation results in eight points at 1.8m above ground, four points along Church Street and four points Gould Street, were calculated (Fig.1). Moreover, the microclimate in eight points on the rooftop of the investigated building (15m above ground, 2m above the rooftop) was assessed to evaluate the effect of the green roof retrofit at the roof level.

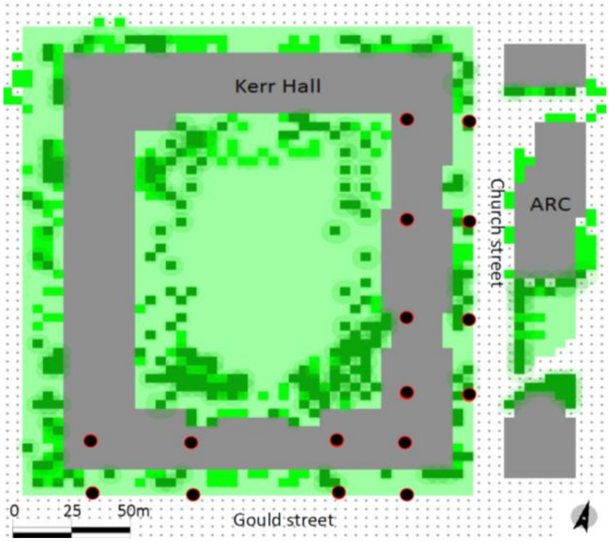

Figure 1. ENVI-met microclimate model with position of the points of analysis (●).

The building energy simulations were then performed using an energy model built in EnergyPlus. In this software, the green roof was modeled using the module developed by Sailor (2008) and corrected by Change (2013). The model is based on the fast all season soil strength (FASST) model of the US Army Corps of Engineers. The module includes long and short wave radiation exchange, sensible heat exchange, thermal and moisture transport in the growing medium, evaporation from the soil, and transpiration from the vegetation. The green roof was modeled as a single vegetation layer on a soil surface. The vegetation was a steady-state semi-infinite plane characterized by an emissivity, albedo, height, and foliage fraction based on the green roof characteristics. In the study the baseline green roof properties were a soil conductivity of 0.4W/mK, a specific heat of 1000J/kgK, and a density of 500kg/m^3 (Sailor et al., 2011).

One of the important aspects while modelling green roofs is that plants have not the same characteristics over time (Moody and Sailor, 2013, Sailor and Hagos, 2011, Ouldboukhitine et al., 2014). For example, the foliage density and the height of the plants are higher in summer compared to winter while the water content, and hence the thermal conductivity, changes frequently. This level of analysis was considered unnecessary for the scope of the present paper.

Electricity data for the investigated building (named Kerr Hall) was acquired for verification of the as is energy model.

CASE STUDY BUILDING

As described in previous sections, green roofs have received increasing attention in Toronto. Moreover, in recent years, an increasing attention to green roofs has raised with the rooftop agriculture movement. As an example, the new Ryerson Engineering building, designed with a 1000 m^2 green roof was recently reconverted in a small farm capable of producing 2 tonnes of food during the summer of 2015 (Ryerson University, 2015). A proposal for installing a green roof on the main Ryerson building was discussed recently (Fig.2).

This building was completed in 1969 and consists of four wing buildings, forming a square which surrounds the Ryerson Community Park. The building hosts both classrooms and office rooms. The building blueprints allowed to know the main enclosure characteristics. In particular, the exterior wall construction consists of a brick veneer facade (12cm), concrete blocks (25cm), XPS layer (4cm), and a final internal gypsum board. The roof construction of the building consists of a bitumen foil, a variable thickness layer (5 to 10 cm), a cork insulation (50mm), and a structural concrete roof (20 cm). The existing roof (not including the green roof) has an R-value of 1.42m^{2}K/W. Following university campus information (Ryerson University, 2014) and the results of an energy audit, typical schedules of use were assumed for the building energy model. The building is heated with steam and cooled with chilled water. Heat exchangers in the building are then used to cool or heat the supply air and distributed through a variable air volume (VAV) systems. In the software, a VAV system with terminal reheat was hence modeled.

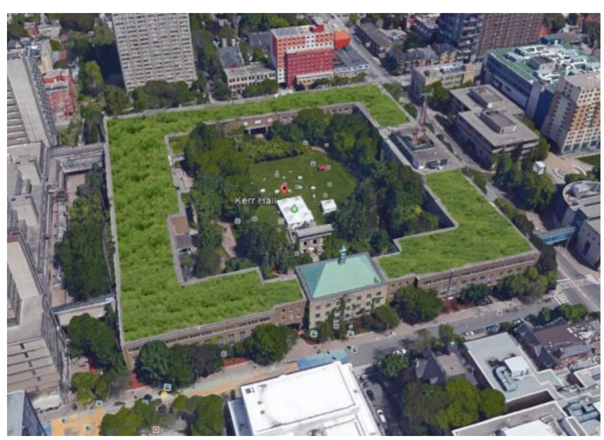

Figure 2. Proposed green roof on the investigated case study building.

Green roofs are often classified in intensive or extensive according to the depth of the soil. Obviously, since extensive green roofs have a shallow growing medium and are lighter, considering the structural capacity of the existing building, an extensive green roof was considered as the only option for this retrofit application. In particular, a structural analysis of the existing roof suggested to limit the additional weight of the green roof to 150 kg/m^2, which corresponds to a regular soil depth of less than 200mm or to a lighted soil medium up to 250mm. By changing the pant selection (also expressed in terms of different Leaf Area Indices) and soil depth, four green roof systems were analyzed. Table 4 lists the main characteristics of the four green roofs that were compared.

Table 4. Characteristics of green roofs investigated as possible retrofitting solutions.

	green roof A	green roof B	green roof C	green roof D
Soil depth, mm	150	150	300	300
Plant height, m	0.5	0.5	0.5	0.5
LAI	1	2	1	2
RSI, m^{2}K/W	1.80	1.80	2.17	2.17

SIMULATION RESULTS

The ENVI-met model was validated using the measured data from local rooftop weather stations. The simulated air temperature on the rooftop was compared to the air temperature data. The difference between the simulation data and measured ones was always below 2°C (with an average value below 0.5°C). This discrepancy could be explained by the inaccuracies in the input parameters for the simulation, such as surface materials, soil, and vegetation conditions (the software only allows to assign a single numerical value to the different materials within the model) or the fact that anthropogenic heat from buildings and cars were not included.

Looking at results in Fig.3, at noon the maximum cooling effect is 0.2˚C and 0.4˚C for green roofs A and B respectively compared to the as is case. At midnight the cooling increases with maximum differences of 0.7˚C and 1.1˚C for green roofs A and B respectively. The decrease in air temperature is due to the evapotranspiration of the vegetation and the increase in albedo of the roof. It is evident that the increase in LAI has a significant impact on the cooling effect at pedestrian level. Air temperature cooling predominantly occurs north-east of the building (Fig.4).

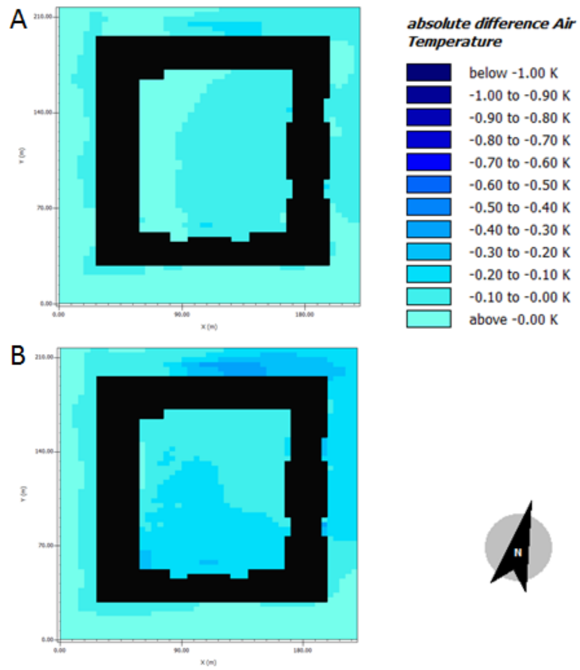

Figure 3. Air temperature difference between green roof A (LAI=1) or green roof B (LAI=2) and as is case, at pedestrian level (1.8m above ground) at 12pm.

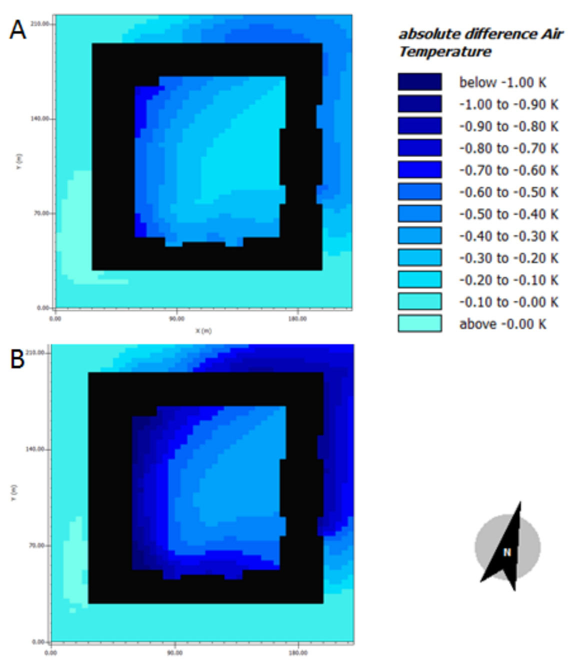

Figure 4. Air temperature difference between green roof A (LAI=1) or green roof B (LAI=2) and as is case, at pedestrian level (1.8m above ground) at 12am.

The MRT proved to be less impacted by the addition of the green roofs (Figs.5 and 6). At noon, there is no significant decrease in MRT for green roof A and a maximum decrease of only 0.2˚C for green roof B. At midnight, the impact on MRT increases slightly to a maximum decrease of 0.1˚C for green roof A and 0.3˚C for green roof B.

After having evaluated the effect at pedestrian level, the study looked at the impact over the roof. The rooftop microclimate may play several roles in outdoor comfort and may also improve HVAC performance due to its free cooling effects, and their resulting lower outdoor air temperatures. The difference in air temperature at the rooftop level for green roof retrofits A (LAI=1) and B (LAI=2), compared to the as is the case at noon and midnight are shown in Fig. 10 and reported in Table 6. While at noon there is minimal difference (green roof retrofit B shows a maximum cooling of 0.4˚C), at midnight the cooling is increased with a maximum reduction of 1.6˚C and 2.6˚C for green roofs A and B respectively. As expected, the impact of the green roof retrofits on the air temperature is more pronounced at the rooftop level. This also agrees with previous studies (Ng et al., 2012, Chen et al., 2009).

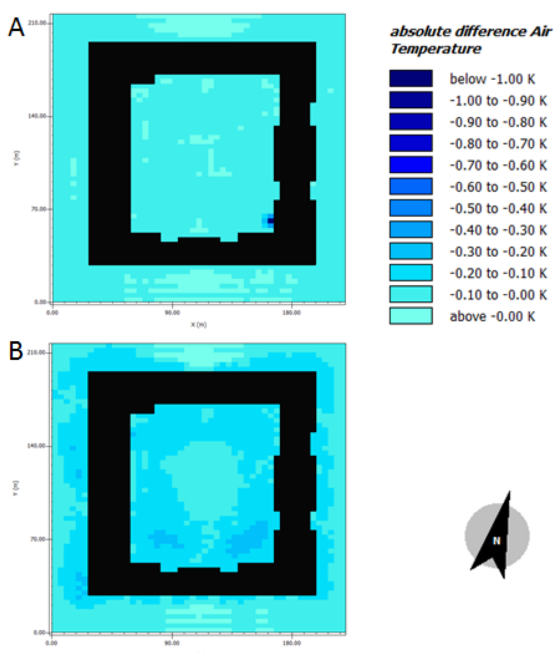

Figure 5. MRT difference between A) green roof A (LAI 1) and as is case B) green roof B (LAI 2) and as is case at 12pm at pedestrian-level (1.8m above ground).

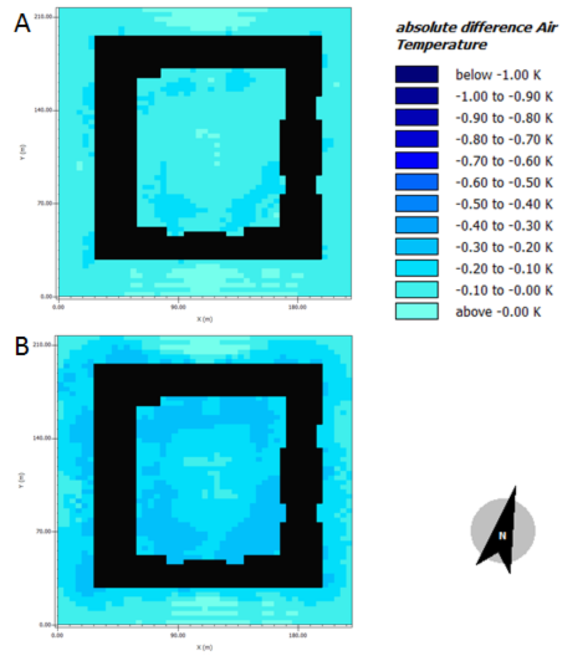

Figure 6. MRT difference between A) green roof A (LAI 1) and as is case B) green roof B (LAI 2) and as is case at 12am at pedestrian-level (1.8m above ground).

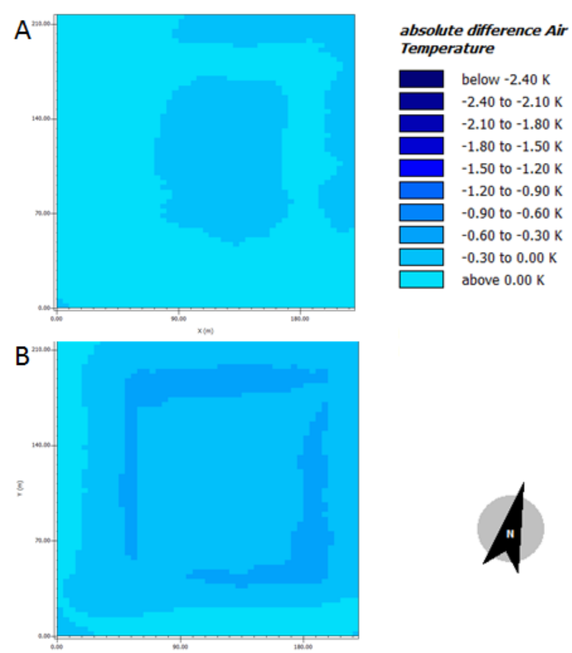

Figure 7. Air temperature difference between A) green roof A (LAI 1) retrofit and as is case and B) green roof B (LAI 2) retrofit and as is case at 12pm at rooftop-level (15m above ground).

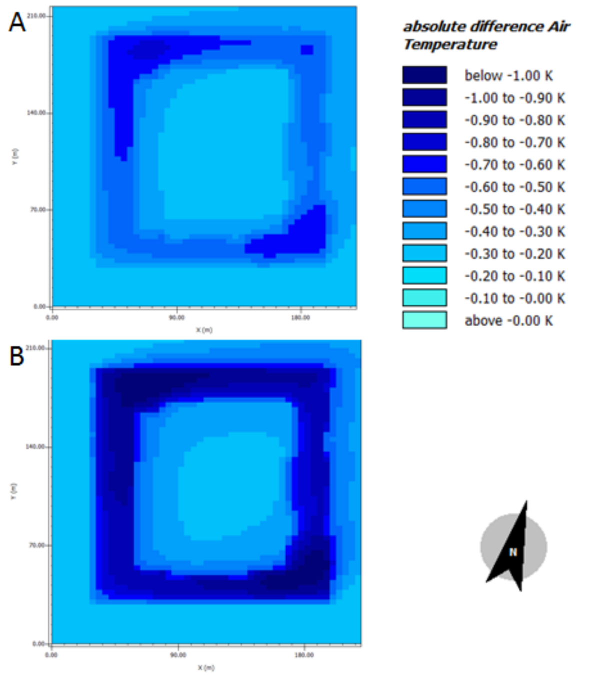

Figure 8. Air temperature difference between A) green roof A (LAI 1) retrofit and as is case and B) green roof B (LAI 2) retrofit and as is case at 12am at rooftop-level (15m above ground).

The energy modelling of the building was hence assessed. The addition of the green roof retrofits A, B, C, and D decreased the EUI to 326kWh/m^2 (-1.7%), 324.9 kWh/m^2 (-2.1%), 323 kWh/m^2 (-2.6%), and 322 kWh/m^2 (-2.9%) respectively. Annual energy savings for gas and electricity along are shown in Fig.9. The simulations resulted in a maximum annual energy savings of 382.6MWh (269.5MWh for gas and 113.1MWh for the electricity) for the retrofit with green roof D. Reduction in heating is the largest contributor to the decrease in energy consumption with energy savings of up to 269kWh (-8.6%) for green roof D compared to the as is case. Reduction in cooling is the second largest contributor with energy savings of up to 78kWh (-4.1%) for green roof D compared to the as is case. Increasing the soil depth from 150mm (green roofs A and B) to 300mm (green roofs C and D) had the largest impact on the energy consumption with a significant savings in heating. Green roofs C and D show significantly more savings in heating with reductions of 8.5% and 8.6% respectively compared to green roofs A and B with reductions of 5.7% and 5.9% respectively. The decrease in heating energy consumption can be attributed to the increase in RSI of the roof from 1.4m^{2}K/W in the as is case to 1.8 m^{2}K/W with the addition of 150mm of soil (green roofs A and B) and 2.17m^{2}K/W with the addition of 300mm of soil (green roofs C and D). The cooling energy consumption was also reduced with the increase in the soil depth. Figure 10 reports the total number of discomfort hours in the third floor for the current building and with the four green roof retrofits, and allows to assess the benefits for the interior comfort too.

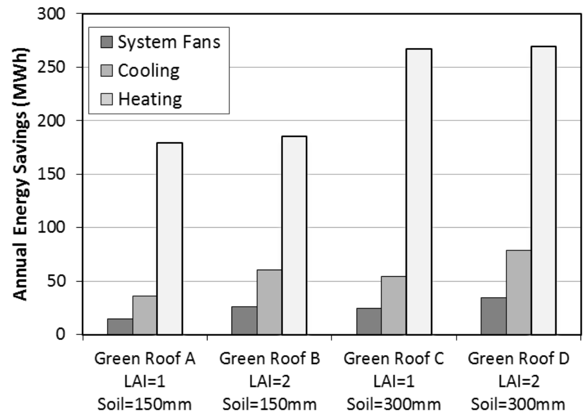

Figure 9. Annual energy savings with the addition of the different green roof retrofits divided by end-use.

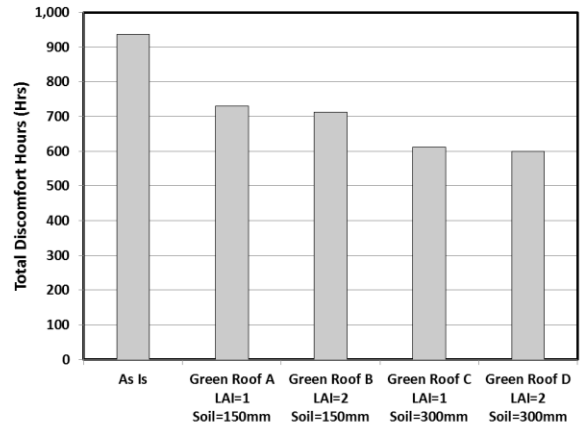

Figure 10. Total number of discomfort hours in the third floor for the as is case and four considered green roofs.

DISCUSSION

The microclimate study has demonstrated that the application of a green roof retrofit on a building in Toronto may decrease the surrounding air temperature by up to 0.4˚C during the day and 0.8˚C at night. These results are comparable to those found in other studies. For example, in New York City afternoon temperatures were found to be reduced by up to 0.6°C with the adoption of green roofs (Savio et al., 2006), while in Hong Kong, air temperatures were reduced by up to 0.7°C at 2pm with green roof applications (Peng and

Jim, 2013). These studies showed slightly larger reductions in air temperatures during the day than the present study, however, they also implemented green roofs on the larger scale of an entire neighbourhood. Although the temperature reduction during the day found in this study is not so significant, it is expected that a larger scale application of green roof retrofits on the campus of Ryerson University would improve even further the outdoor thermal comfort.

The energy model results proved that the addition of a green roof on Kerr Hall may decrease the EUI by 5.8 kWh/m^2 to $9.6kWh/m^2$. This is slightly higher than the assumed energy savings of $4.15kWh/m^2$/year in the Toronto that was used by Banting et al. (2005). According to the study conducted by Niachou et al. (2001) in Athens, Greece, a moderately insulated building such as Kerr Hall would result in a heating savings of 13%, cooling savings of 0-4%, and total energy savings of 3-7%. For this study very similar results were found with maximum heating saving of 9%, cooling saving of 4%, and total energy saving of 3% with green roof retrofit D.

In a study by Sailor et al. (2012), nine green roofs in four cities were modeled on new buildings designed according to the standard ASHRAE 90.1, and it was found that while LAI is an important parameter in regards to cooling, green roofs in cold climates result in larger energy savings due to the heating demand, and the saving is largely impacted by the soil depth. Out of the four cities considered in that study, New York has the closest climate to that of Toronto, and showed a gas saving of $20,000kJ/m^2$, while in the present study a gas saving of $50,695kJ/m^2$ was obtained with the addition of the green roof retrofit B. The difference between the studies can be attributed to the differences in building characteristics and climate. As shown by Niachou et al. (2001), the energy savings of green roofs highly depends on the existing roof insulation levels with lower levels of insulation resulting in larger energy savings. As the focus of the present study was for the green roof retrofit of a relatively poorly insulated building, the results obtained were considered highly satisfactory.

CONCLUSIONS

In this study, the effects of a green roof retrofit on the outdoor microclimate and energy consumption of the main building of the Ryerson University in Toronto were investigated. The cooling effect on the urban microclimate with green roof retrofits increased with the increase of the LAI. At pedestrian level the cooling pattern followed the wind prevalent directions. An average reduction in peak temperature up to 0.4˚C and 0.7˚C for green roofs with a LAI of 1 or 2 respectively was found, although no appreciable effect was obtained for the MRT at pedestrian level. Reversely, at the rooftop level, the cooling effects were larger. Peak air temperature reductions of 0.4˚C and 0.8˚C during the day and of 1.1˚C and 2.0˚C at night were found.

The building energy consumption after the retrofitting was found more influenced by the soil depth than by the LAI of the green roof. Total energy reductions of 1.8% to 2.9% were modeled. The reduction in heating on the last floor of the building was the largest contributor to the overall energy saving. The cooling demand was found to be most impacted by LAI. The decrease in cooling demand with increased LAI was directly linked to the decrease in roof surface temperature. Discomfort hours were found to be largely impacted by the soil depth. A reduction of the discomfort hours between -22% and -36% for the different green roof options resulted on the last level of the building.

In conclusion, this paper has shown that a green roof retrofit could have an appreciable impact on the outdoor microclimate while resulting in energy savings too. However, in this study, two different models were created for the different simulations. The hope is that in the near future, energy modelling will allow to interact with urban modelling more closely, as this last seems to attract an increasing attention, not only for architects and designers, but also for city planners, policy makers and for the large community of building citizenships.

ACKNOWLEDGEMENTS

This research was funded by the Centre for Urban Research (CUR) of Ryerson University through the project "Policy Guidelines for Increasing Outdoor Thermal Comfort in Toronto: An Analysis of the Urban Microclimate". The author expresses his gratitude to Prof. Michael Bruse for providing the ENVI-met software and to Melissa Furukawa for having developed the ENVI-met model as a part of her Master thesis.

REFERENCES

Alexandri E., Jones P. (2008). Temperature decreases in an urban canyon due to green walls and green roofs in diverse climates. *Building and Environment*, 43(4), 480–493.

Banting D., Doshi H., Li J., Missios P., Au A., Currie B.A., Verrati M. (2005). Report on the Environmental Benefits and Costs of Green Roof Technology for the City of Toronto.

Berardi U., GhaffarianHoseini A., GhaffarianHoseini A. (2014) A critical analysis of the environmental benefits of green roofs. *Applied Energy*, 115, 411–428.

Bruse M. (2015). ENVI-met website: www.envimet.com

Castleton H.F., Stovin V., Beck S.B.M., Davison J.B. (2010). Green roofs; building energy savings and the potential for retrofit. *Energy and Buildings*, 42, 1582–1591.

City of Toronto. (2015). Green Roofs. Retrieved from: http://www1.toronto.ca/wps/portal/contentonly?vgnextoid=3a7a036318061410VgnVCM10000071d60f89RCRD

Maloley M.J. (2009). Land surface temperature mapping of the greater Toronto area from Landsat TM/ETM+ thermal imagery: 1987-2008. Report, Canada Centre for Remote Sensing. Natural Resources Canada.

Moody S.S., Sailor D.J. (2013) Development and application of a building energy performance metric for green roof systems, *Energy and Buildings*, 60, 262–269.

Niachou A., Papakonstantinou K., Santamouris M., Tsangrassoulis A., Mihalakakou G. (2001). Analysis of the green roof thermal properties and investigation of its energy performance. *Energy and Buildings*, 33 (7), 719-729.

Ouldboukhitine S.E., Belarbi R., Sailor D.J. (2014). Experimental and numerical investigation of urban street canyons to evaluate the impact of green roof inside and outside buildings. *Applied Energy*, 114, 273–282.

Ozkeresteci I., Crewe K., Brazel A.J. (2003). Use and evaluation of the ENVI-met model for environmental design and planning: an experiment on linear parks. Proc. of the 21st International Cartographic Conference.

Parizotto S., Lamberts R. (2011). Investigations of green roof thermal performance in temperature climate: A case study of an experimental building in Florianopolis city, Southern Brazil. *Energy and Buildings*, 43, 1712–1722.

Peng L.L.H., Jim C.Y. (2013). Green-Roof Effects on Neighborhood Microclimate and Human Thermal Sensation. *Energies*, 6, 598-618.

Ryerson University. (2014). Energy Conservation and Demand Management Plan.

Ryerson University. (2015). Sustainability Program Facts. http://www.ryerson.ca/campusfacilities/departments/sustainability/index.html#tab2

Saadatian O., Sopian K., Salleh E., Lim CH.., Riffat S., Saadatian E., Toudeshki A., Sulaiman M.Y. (2013). A review of energy aspects of green roofs. *Renewable and Sustainable Energy Reviews*, 23, 155–168.

Sailor D.J, Hagos M. (2011). An updated and expanded set of thermal property data for green roof growing media, *Energy and Buildings*, 43(9), 2298–2303.

Sailor D.J. (2008). A green roof model for building energy simulation programs. *Energy and Buildings*, 40, 1466-1478.

Sailor D.J., Elley T.B., Gibson M. (2012). Exploring the building energy impacts of green roof design decisions – a modeling study of buildings in four distinct climates. *Journal of Building Physics*, 35 (4), 372-391.

Santamouris M. (2014). Cooling the cities – A review of reflective and green roof mitigation technologies to fight heat island and improve comfort in urban environments. *Solar Energy*, 103, 682-703.

Savio P., Rosenzweig C., Sokecki W.D., Slosberg R.B. (2006). Mitigating New York City's Heat Island with Urban Forestry, Living Roof, and Light Surfaces. New York City Regional Heat Island Initiative. The New York State Energy Research and Development Authority, Albany, NY.

UFRED, Urban Forest Research and Ecological Disturbance Group. (2015). Tree species map of Ryerson Community. Parktrees. Retrieved from: http://parktrees.ca/

Wang Y., Berardi U., Akbari H. (2016). Comparing the effects of urban heat island mitigation strategies for Toronto, Canada. *Energy and Buildings*, 114, 2-19.

Wang Y., Berardi U., Akbari H. (2015). The Urban Heat Island effect in the city of Toronto. *Procedia Engineering*, 118, 137-144.

Wieditz I., Penney J. (2007). Time to tackle Toronto's warming: climate change adaptation options to deal with heat in Toronto. Clean Air Partnership.